



since 1961

Baltica

BALTICA Volume 36 Number 2 December 2023: 164–175

<https://doi.org/10.5200/baltica.2023.2.6>

The dynamics of Pilkosios Dunes relief during 2010–2022, based on the digital elevation model analysis

*Gabrielė Tijūnaitytė**, *Simonas Danielius*, *Linas Bevainis*, *Jonas Satkūnas*, *Lauras Balakauskas*

Tijūnaitytė, G., Danielius, S., Bevainis, L., Satkūnas, J., Balakauskas, L. 2023. The dynamics of Pilkosios Dunes relief during 2010–2022, based on the digital elevation model analysis. *Baltica*, 36 (2), 164–175. Vilnius. ISSN 0067-3064. Manuscript submitted 27 September 2023 / Accepted 22 November 2023 / Available online 14 December 2023

© Baltica 2023

Abstract. To assess aeolian relief dynamics in Pilkosios Dunes, 6 digital elevation models (DEMs) were prepared from the year 2010, for January, May and October of 2018, for May of 2019, and for November of 2022. These DEMs were then compared with each other to obtain elevation difference rasters through time. The obtained results indicated that elevation changes were directional through time, and their highest intensity coincided with the bare-sand surface class, where active blowout landforms were located. In these locations, the average negative elevation change rate was determined to be approximately 2 cm/year. To analyse the driving forces of these elevation changes, the relationships between a measure of elevation change and the tested factor characteristics were evaluated. The strongest relationship amongst all tested factors was found with the distance to the edge of grassland/bare sand. Locations that were farther away from this edge experienced a four times larger decrease in elevation, compared to areas closer to the edge. The distance to the shoreline, which is related to the absolute altitude, was also an important factor. This relationship can be summarized as follows: the lowest areas, which were further from the lagoon, were inactive; while the highest locations, which were closer to the shoreline, had the highest intensity of elevation change (averaging 0.5–0.7 m for adjacent to the shoreline locations and -1.7 m for locations ~ 300 m away from the shoreline). The slope factor described a trend of how the steepest slopes were decreasing in height by 2 m on average, while gentler slopes were mostly stable.

Keywords: *photogrammetry; The Great Dune Ridge; UAV; aeolian dynamics*

✉ *Gabrielė Tijūnaitytė** (Gabriele.tijunaityte@gmail.com),  <https://orcid.org/0009-0006-5916-284X>,

Linas Bevainis  <https://orcid.org/0000-0001-9860-4440>,

Lauras Balakauskas  <https://orcid.org/0000-0002-8941-989X>

Vilnius University, Faculty of Chemistry and Geosciences, Institute of Geosciences, M.K. Čurlionio str. 21/27, 03101 Vilnius, Lithuania

Simonas Danielius, Jonas Satkūnas  <https://orcid.org/0000-0001-9086-8038>

Nature Research Centre, Institute of Geology and Geography, Akademijos str. 2, 08412 Vilnius, Lithuania

*Corresponding author

INTRODUCTION

The Curonian Spit is a major part of the Lithuanian coastline. It is recognized as a UNESCO World Heritage Site for its unique landscape depicting interactions between wind, water, and human activities. Although currently, the Curonian Spit is mostly stable, composed of forest-fixed dunes (Bučas 2007; Česnulevičius *et al.* 2006; Mardosienė 1989), throughout its history the relief of the Curonian Spit

went through dramatic changes, some of which were due to human interventions, mostly land use change from the forest to pasture fields and back to reforested areas again (Buynevich *et al.* 2015; Dobrotin *et al.* 2013; Gudelis 1998; Gudelis, Michaliukaitė 1959; Michaliukaitė 1967; Moe *et al.* 2005; Savukyniene *et al.* 2003). The history of the Curonian Spit and its development according to human management decisions show that human actions can cause rapid consequences and the understanding of the dynamics

of dunes on a short-time scale is vital for effective coastal management.

Most of the aeolian dynamics studies in the Pilkosios Dunes have so far been confined to cartometric surveys or comparisons of quantitative measurements and qualitative descriptions in fieldwork settings (Berendt 1869; Česnulevičius *et al.* 2006, 2017; Mardosienė 1989; Michaliukaitė 1967; Morkūnaitė 2000; Morkūnaitė, Česnulevičius 2005), as well as the use of satellite images to estimate volumetric changes (Povilanskas 2009; Povilanskas *et al.* 2006, 2009). These data provide very limited means to assess the spatial properties of relief dynamics. A much better coverage and resolution can be achieved using modern remote sensing techniques, such as UAV-aided photogrammetry or LiDAR collected data (Le Mauff *et al.* 2018; Pucino, Conduro 2016; Suo *et al.* 2017; Taddia *et al.* 2017). However, UAV use for the studies of aeolian morphodynamics in the Curonian Spit have been extremely limited thus far (Česnulevičius *et al.* 2019; Morkūnaitė *et al.* 2018). The UAV-based methodology allows a much more effective data collection, compared to that of earlier studies (Gonçalves, Henriques 2015; Guillot, Pouget 2015). In addition, DEMs compiled as a result of such investigations enable a more detailed analysis and evaluation of the effects of various parameters influencing morphodynamics.

In this study, several high spatial resolution and large aerial coverage DEMs were prepared for the active part of Pilkosios Dunes for the years 2010, 2018, 2019 and 2022 to investigate elevation changes and to determine the major factors responsible for these elevation changes.

DATA AND METHODS

The study area (Fig. 1) was confined to the active part of Pilkosios Dunes. The active part was determined based on available information about dune activity in literature (Česnulevičius *et al.* 2006; Morkūnaitė, Česnulevičius 2005).

All data processing was carried out using ArcGIS

Pro 3.0 software. To obtain surface type data in the study area, the supervised classification (using Random Tree Classifier model) was applied on the digital raster orthophoto map ORT10LT_2020 provided by the National Land Service under the Ministry of Environment (from www.geoportal.lt). The training areas were manually prepared for three dune surface classes: tree canopies, bare sand, and grassland.

In this study, a total of 6 DEM elevation datasets, representing time periods listed in Table 1 were prepared for further analysis. All DEM rasters were resampled to the matching (2 m × 2 m) resolution, ensuring the snapping of the grid cells among rasters.

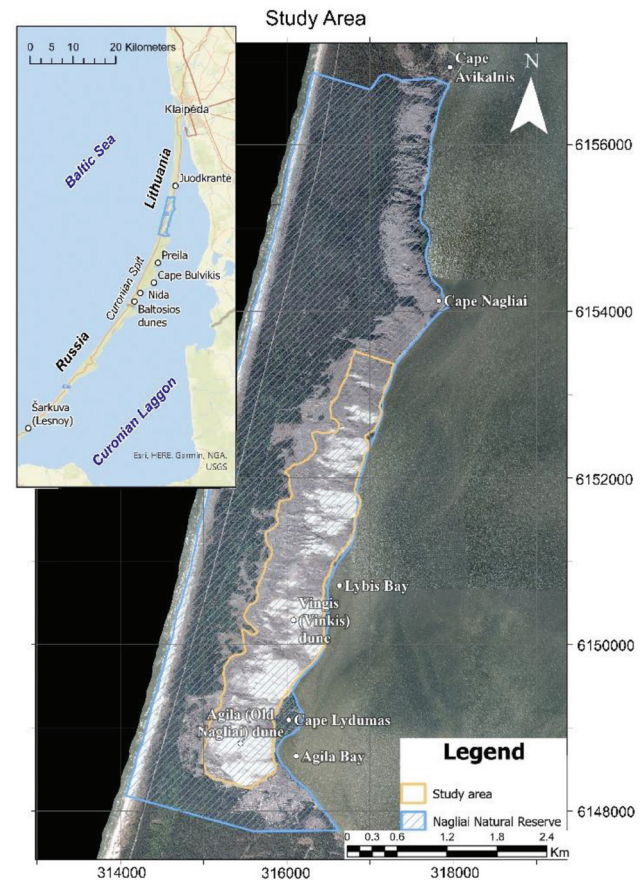


Fig. 1 The study area, coordinate system: LKS 1994 (Orthophoto map © Nacionalinė žemės tarnyba prie Aplinkos ministerijos)

Table 1 Properties of DEMs used in this study

Date of data collection	Name of produced DEM	Acquisition type	Initial spatial resolution
Jun/Sept 2010	DEM100x	Created from the LiDAR point cloud provided in ASCII XYZ format by the National Land Service under the Ministry of Environment.	2 m × 2m
8 Jan 2018	DEM1801	Obtained using data from Sense Flye Bee UAV connected to RTK ("LitPOS" network) and calculated based on Structure-from-Motion (SfM) algorithm (Fonstad <i>et al.</i> 2013), using the <i>eMotion</i> [3.5] and <i>Pix4Dmapper</i> software programs.	4.02 cm × 4.02 cm
10 May 2018	DEM1805		3.94 cm × 3.94cm
17 Oct 2018	DEM1810		3.90 cm × 3.90 cm
22 May 2019	DEM1905		3.84 cm × 3.84 cm
2 Nov 2022	DEM2211	Obtained using data from DJI Phantom Pro RTK UAV connected to RTK ("LitPOS" network), calculated using photogrammetric software "Pixpro".	6.58 cm × 6.58 cm

For the modelling of changes through time, the DEMs of consecutive time periods were compared by subtraction, thus producing difference rasters.

For a preliminary assessment of the main factors that lead to elevation changes, correlation coefficients were calculated between elevation difference and different properties influencing relief dynamics. Two variants of elevation difference rasters were used: a) the elevation difference raster between the earliest and the latest DEMs in the study ($DEM_{2211} - DEM_{100x}$) (Fig. 2a) and b) the raster with moduli values of these elevation differences ($|DEM_{2211} - DEM_{100x}|$) (Fig. 2b). The latter represents the magnitude of elevation difference; and the former, both magnitude and type (accumulation or deflation).

Both elevation changes and their moduli were compared with the following properties of the study area (Fig. 3): a) absolute altitude (DEM_{100x} , representing the absolute elevation at time zero), b) relative elevation, c) distance to the shoreline of the Curonian Lagoon, d) distance to the edge of the bare-sand surface class, e) slope direction relative to W direction, representing windward and downwind slopes (Česnulevičius *et al.* 2017; Morkūnaitė *et al.* 2018; Paškauskas 2006), and f) slope (calculated from DEM_{100x}). Relative elevation was calculated from the DEM_{100x} by subtracting from the original cell's value the mean value within a radius of 5, 10, 20, 40, 50, 60, 80, 200, 400, 450, 500, 550 or 600 cells of this cell.

Ten thousand random points were generated within the bare-sand surface class, and the values of raster

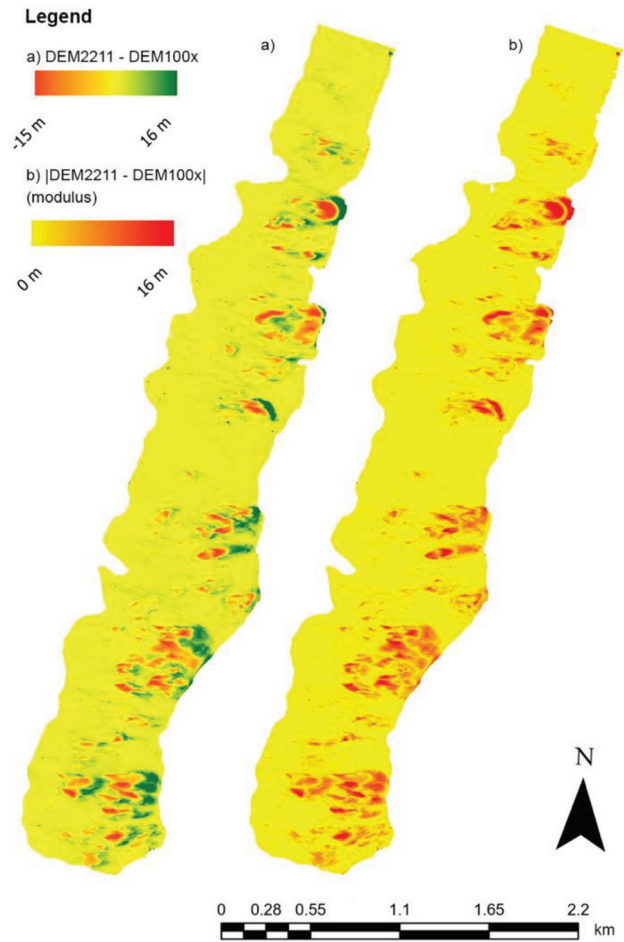


Fig. 2 A measure of elevation change: a) elevation difference raster ($DEM_{2211} - DEM_{100x}$), b) the modulus of elevation difference raster ($|DEM_{2211} - DEM_{100x}|$)

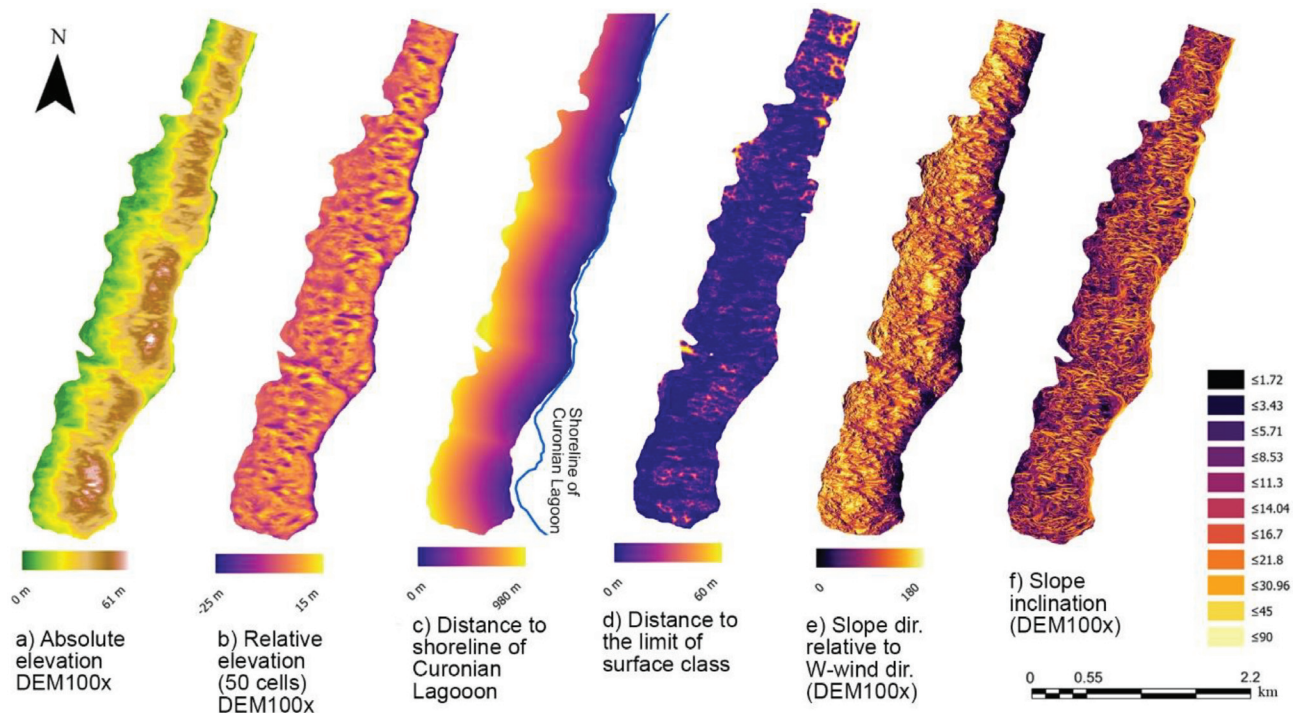


Fig. 3 Assessed factor rasters

datasets were extracted to these points of both measures of elevation change, as well as all the above-mentioned factors (a–f). Pearson’s r coefficient was calculated for the compared pairs of properties. The coefficients higher than ~ 0.026 can be considered significant with alpha of 1% (Obilor, Amadi 2018). After each r calculation, to visualize the found trends, each property raster was reclassified into intervals of analysed characteristics and the average values of elevation change were calculated for each of these intervals.

RESULTS

According to the ORT10LT (Fig. 1) classification, grassland was the most extensive surface class (58.6%) in the study area, followed by the bare-sand surface class, which covered 40.2% of the area. The remaining 1.2% of cells were classified as tree canopies. It is evident that bare-sand surfaces were more dominant on the E part of the ridge and were more extensive in the S part compared to the N part of the study area.

Visually, all the compiled DEMs are similar. The absolute elevation ranged within the interval of 0–62 m a.s.l. The W side of the study area was, on average,

lower (~ 11 m a.s.l), while the E part was, on average, higher (~ 33 m a.s.l), i.e., the ridge was situated in the latter. The windward slope of the ridge averaged $2\text{--}7^\circ$, and the leeward slope averaged $\sim 16^\circ$. The maximum calculated slope was $\sim 58^\circ$. The average elevation of each time period is presented in Fig. 4.

A comparison of the corresponding DEM surfaces showed that most of the study area had a negligible elevation difference (close to zero), which was expected, as the grassland class area can be consid-

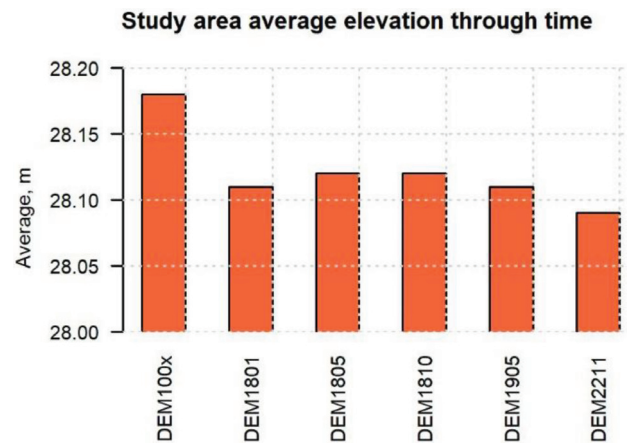


Fig. 4 The dynamics of average elevation in the study area

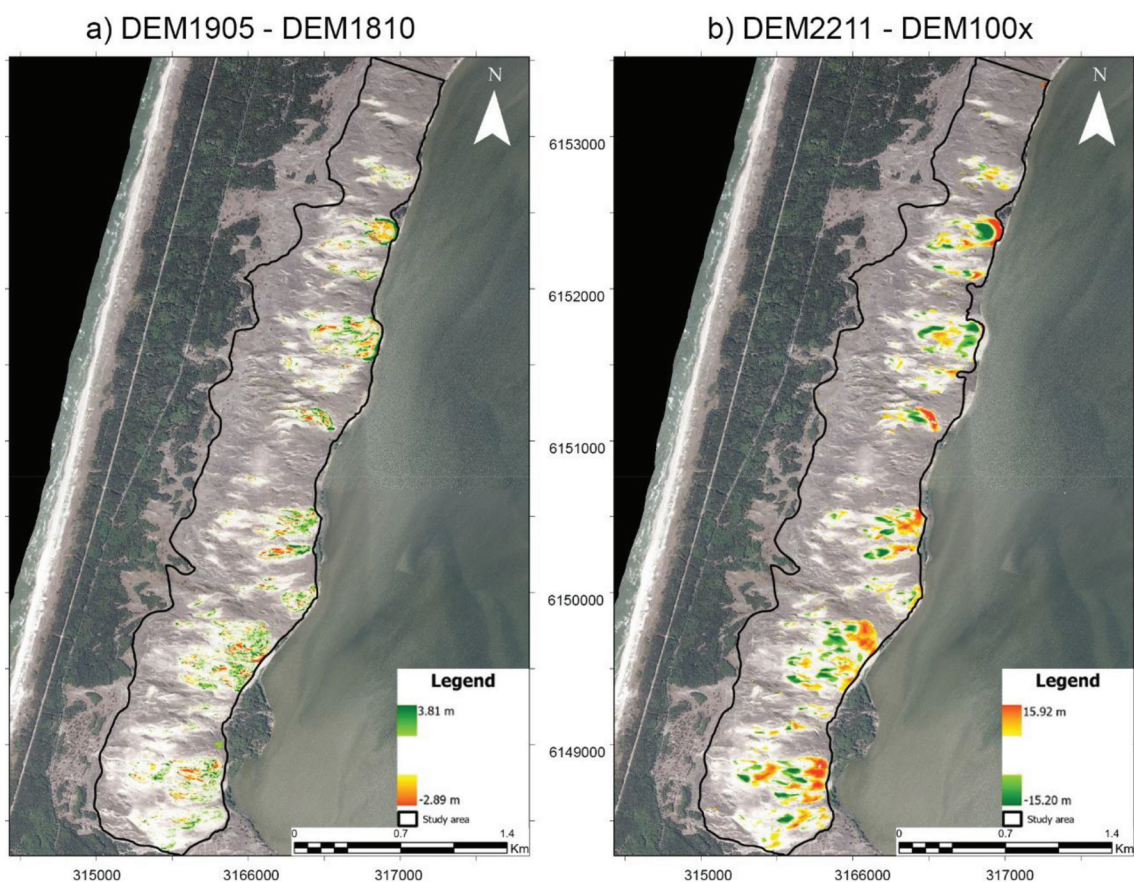


Fig. 5 Elevation differences based on the length of time of measurements: a) short time interval represented by *DEM1905-DEM1810* elevation difference; b) longer time interval represented by *DEM2211-DEM100x*. Coordinate system: LKS 1994. (Orthophoto map © Nacionalinė žemės tarnyba prie Aplinkos ministerijos)

ered stable (Česnulevičius *et al.* 2006; Morkūnaitė, Česnulevičius 2005). Nevertheless, areas of high-intensity elevation changes can be identified as well (Fig. 5). In these areas, elevation differences were ranging from a few meters (on a short-time scale) up to approx. 15 m (throughout the whole studied time interval) (Table 2). The positive elevation differences were mostly concentrated on the E side of blowouts, coinciding with the lee slopes of accumulation lobes, where the most intense elevation gain takes place usually in the middle of the whole accumulation zone (i.e., in the middle of a slope). The largest elevation losses were on the stoss slope of deposition lobes, near erosive deflation edges of blowouts, and at the bottom of blowouts, usually concentrated on the W part of a blowout.

Within a shorter interval of time, differences were less significant (Fig. 5a), e.g., in elevation differences from years 2018–2019, the maximum elevation loss was up to 3.29 m, while elevation gain reached up to 5.31 m (Table 2). However, the elevation change rate was not constant over time. Some of the difference rasters represent similar lengths of time but different seasons of the year: *DEM1805-DEM1801* represents elevation differences during 4 winter–spring months, and *DEM1810-DEM1805* represents differences during 5 summer-autumn months. The latter raster

appears to be less stable – elevation changes in the same locations were higher compared to the difference raster representing winter and spring months. In addition, *DEM1810-DEM1805* has a higher standard deviation (Table 2). The long-term elevation changes (i.e., *DEM2211-DEM1905*, *DEM2211-DEM100x*, Fig. 5b) appear to be more widespread throughout the bare-sand surface class. In these datasets, the maximum elevation decrease could reach 15.20 m, and increase could be up to 15.63 m (Table 2). In addition, on a longer-time scale, the standard deviation of elevation difference was larger, meaning that more locations differed from the average elevation difference, which was close to 0 m. It can also be noted that the average elevation difference within the bare-sand surface class was negative (Table 3).

The calculated *r* coefficients for factors influencing dune dynamics ranged from -0.36 to 0.47, some being close to 0 (Table 4).

When comparing the average modulus of elevation difference values between different distances to the edge of the bare-sand surface class (Fig. 6a, orange colour) we found that areas that were farther away from the edge of the bare-sand surface class predominantly experienced larger elevation changes. These changes could reach up to 5 m for the areas furthest from the class edge. Accordingly, the distance to the edge of

Table 2 Elevation difference rasters and their minimum and maximum values for the whole study area

Elevation difference raster	Elevation difference (m)			
	Min	Max	Mean	Std
<i>DEM1801-DEM100x</i>	-11.48	12.64	-0.05	1.32
<i>DEM1805-DEM1801</i>	-2.64	2.63	0.01	0.10
<i>DEM1810-DEM1805</i>	-3.29	5.31	0.00	0.14
<i>DEM1905-DEM1810</i>	-2.89	3.81	0.00	0.15
<i>DEM2211-DEM1905</i>	-9.88	11.03	-0.02	0.74
Combined time interval (<i>DEM2211-DEM100x</i>)	-15.20	15.93	-0.09	1.85

Table 3 The average values for elevation difference and the modulus of elevation difference in the bare-sand surface class

Length of time interval	Elevation difference	Average value in the bare-sand surface class (m)
4 months	<i>DEM1805-DEM1801</i>	0.02
	<i>DEM1805-DEM1801</i>	0.09
7.5 years	<i>DEM1801-DEM100x</i>	-0.17
	<i>DEM1801-DEM100x</i>	1.24
12 years (the combined interval)	<i>DEM2211-DEM100x</i>	-0.29
	<i>DEM2211-DEM100x</i>	1.77

Table 4 Calculated correlation coefficients

Environmental parameter	<i>DEM2211-DEM100x</i>	<i>DEM2211-DEM100x</i> (modulus)
Distance to the edge of the bare-sand surface class	-0.34	0.47
Distance to the shoreline	-0.06	-0.36
Relative elevation	-0.34 (50 cells)	0.25 (800 cells)
Absolute altitude	-0.19	0.25
Slope direction	-0.19	-0.22
Slope	-0.02	0.08

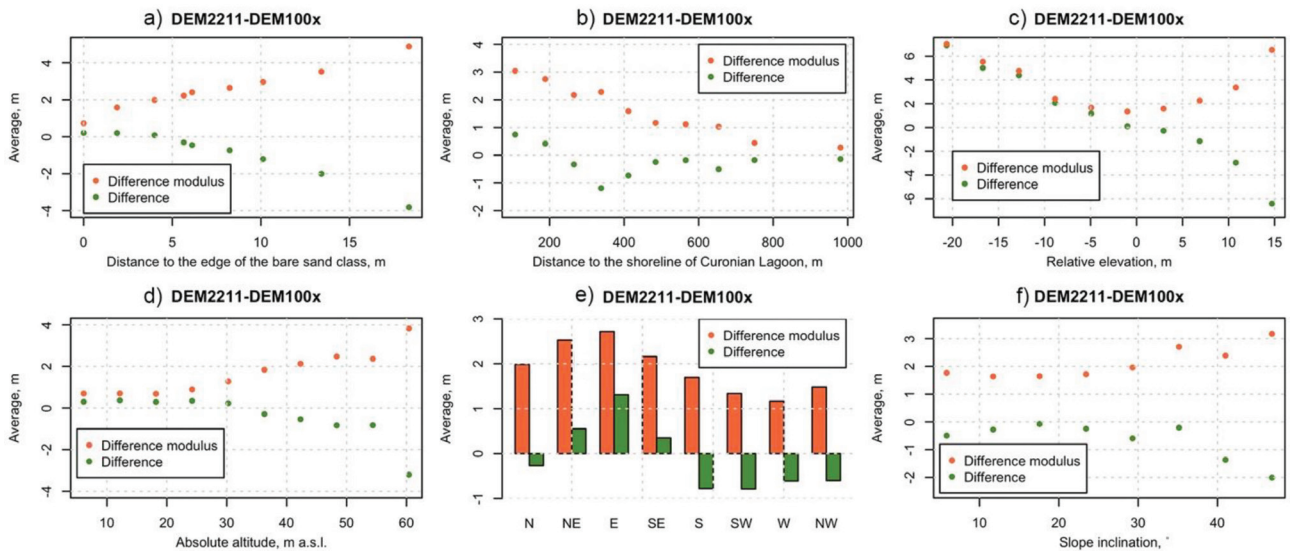


Fig. 6 The average values of elevation difference and the modulus of elevation difference in relation to a) the distance to the edge of the bare-sand surface class (classified into percentiles), b) the distance to the shoreline of the Curonian Lagoon group (classified into percentiles), c) relative elevation, which was calculated using a neighbourhood of 50 cells, group (classified into 10 equal-length intervals), d) absolute altitude group (classified into 10 equal-length intervals), e) different slope orientation, and f) different slope (classified into percentiles)

the bare-sand surface class had the strongest calculated correlation coefficient among all tested factors, indicating the strongest relationship (Table 4).

A comparison of the average values of elevation difference with each distance to the edge of the bare-sand surface class group (Fig. 6a, green colour) confirms a negative relationship found with elevation difference: the locations closer to the edge of the bare-sand surface class have marginal changes, compared to farther locations. The locations farthest from this edge are predominantly decreasing in height (the average reaches 4 m).

There was a negative relationship observed between the distance to the shoreline of the Curonian Lagoon and the modulus of elevation difference (Fig. 6b, orange colour). Closer to the shoreline areas experienced 1.5–3 m elevation change on average, and the elevation change of farthest areas was close to 0 m. This is also indicated by the second strongest, negative r coefficient among all tested factors (Table 4). When comparing the average values of elevation difference (Fig. 6b, green colour) with the distance to the shoreline of the lagoon, no clear trend was observed: adjacent to the shoreline areas were increasing in height (average up to 1 m), areas further by approx. 200 m from the shoreline were decreasing in height, and the farthest areas (500 m and further) were relatively stable.

The strongest correlation coefficient between elevation difference and relative elevation was obtained when relative elevation was calculated using a radius of 50 cells (Fig. 7). Locations lying at higher altitudes than their surrounding areas (within this radius) are most likely to decrease in height (by 6 m on average),

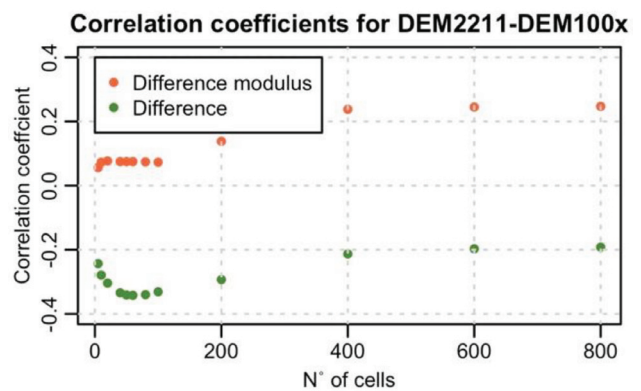


Fig. 7 Correlation coefficients between relative elevation (calculated with different neighbourhood sizes) and elevation difference and its modulus value

while the locations lying at lower altitudes than their surrounding areas are expected to increase in height (by 6 m on average) (Fig. 6c, green colour). This is also observed in correlation coefficients between elevation difference and relative elevation, where the calculated r was -0.34 (Table 4). The averages of the modulus of elevation difference in relation to different relative elevation groups (Fig. 6c, orange colour) show that areas lying higher or lower than their surrounding areas experienced the similar intensity of average elevation change. Correlation coefficients between relative elevation and the modulus of elevation difference were ranging from -0.02 to 0.34 when different radii were used to obtain the relative elevation data (Fig. 7). The highest r values were obtained using a radius of 600 cells. However, at large radii the relative elevation effects did not differ significantly from those of absolute elevation.

A positive relationship was evident between absolute altitudes and the modulus of elevation change (Fig. 6d, orange colour): in the areas of higher altitude, the average modulus of elevation difference could reach up to 4 m, while at lower altitudes such modulus was close to zero. This is also evident in the calculated positive r coefficient ($r = 0.25$) (Table 4). When comparing the average values of elevation difference with different absolute altitudes (Fig. 6d, green colour), it can be noted that higher areas primarily experienced larger and negative elevation differences (this was clear above 20 m a.s.l.; Fig. 6d). The calculated r coefficient between absolute altitude and elevation difference was equal to -0.19 , indicating a negative relationship (Table 4).

A pattern can be seen in the averages of the modulus of elevation difference in relation to cardinal directions (Fig. 6e, orange colour): the largest average values were for the E-, NE-, and SE-facing slopes (~ 2.7 m) and the lowest for W and SW slopes (~ 0.5 m). When the elevation difference values (not its modulus) were averaged for each cardinal direction (Fig. 6e, green colour), E-facing slopes were found to be predominantly increasing in height (~ 1.4 m on average), and S–SW–W–NW slopes were decreasing (~ 0.7 – 0.6 m). All calculated r values with the slope direction relative to W winds were negative. The strongest relationship was found with the modulus of elevation difference ($r = -0.22$). This negative r coefficient indicates a trend that E-facing slopes experienced more intense elevation changes.

When comparing the modulus of elevation difference with slope (Fig. 6f, orange colour), firstly it can be noted that all areas with a non-zero slope independently of the inclination angle were predominantly decreasing in height. This average decrease in height was the lowest for slopes of $\sim 17^\circ$ – 21° , as well as $\sim 35^\circ$. No strong relationships were observed between the slope and elevation difference (the r coefficients were close to 0) (Table 4). When comparing the modulus of elevation difference with slope (Fig. 6f, green colour), the following trend could be observed: the modulus was increasing with the slope, which was also evident by an estimated somewhat stronger relationship with the modulus value of elevation difference (r equal to 0.08, Table 4).

DISCUSSION

The significant elevation changes in the study area coincide with bare-sand surfaces. This is because surfaces without vegetation cover are more vulnerable to deflation processes compared to overgrown surfaces. Many researchers have identified vegetation cover as one of the most important factors in aeolian dynamics (Gares, Nordstrom 1995; Gonçalves, Henriques

2015; Michaliukaitė 1967). Vegetation cover reduces the momentum of wind and lowers its erosional power, also covers sediments, and directly protects the surface (Nickling, Neuman 2009). In addition, vegetation acts as a trap for transported sand particles and reduces any further sand migration (Van de Ven *et al.* 1989; Wolfe, Nickling 1993). Effects of vegetation have also been noted by researchers working in the study area (e.g., Česnulevičius *et al.* 2006; Michaliukaitė 1967). The influence of vegetation also has spatial patterns within the bare-sand surface class. As noted in the Results section, the further the locations are from the edge of grassland/bare-sand classes, the more active they are, and this activity is usually evidenced as a decrease in elevation. Apparently, vegetation reduces wind momentum in the immediate vicinity of the boundary areas, thus reducing the wind's erosive power even on the bare-sand surfaces.

The vegetation cover could also act as a catchment area of migrating sediment, but for this, sediment supply is crucial (Hesp 2011a; Nickling, Neuman 2009). In the study area, sediment supply from outside the system is impossible due to forests in “palvė” (to the W side of the Great Dune Ridge) separating a possible source of fresh sediments – Baltic Sea beach – from the Great Dune Ridge (Fig. 8) (Česnulevičius *et al.* 2006; Gudelis, 1998; Povilanskas *et al.* 2009).

The distance to the shoreline of the Curonian Lagoon could be a descriptor of spatial patterns for dune dynamics. Based on the negative correlation coefficients (Table 4), as well as on the distribution of averages of elevation difference for each distance to the Curonian Lagoon group (Fig. 6b), it can be summarized as follows: the localities farthest from the shoreline are relatively stable. This could be due to a larger proportion of overgrown surfaces on the W side, which, as mentioned above, acts as a stabilizing agent, or due to the adjacent forests in “palvė” (Fig. 8), which not only cut off sand transport from the Baltic Sea beach but also protect the lower W section of the ridge from the predominant W winds (Česnulevičius *et al.* 2017; Morkūnaitė *et al.* 2018; Paškauskas 2006) and their erosional effects, while exposing the middle part of the ridge to these winds. These erosional effects can be seen when comparing the average values of elevation difference for each elevation group (Fig. 6b), as approx. 230–400 m away from the shoreline these averages are negative. The areas lying closer to the shoreline experience larger elevation differences that are mostly positive. These are the E slopes of the Great Dune Ridge (Fig. 8), where sand accumulation takes place, as it is common for the lee slopes of the dunes (Anderson 1988; Hesp 2002). Based on the distance from the shoreline of the Curonian Lagoon, it is possible to distinguish

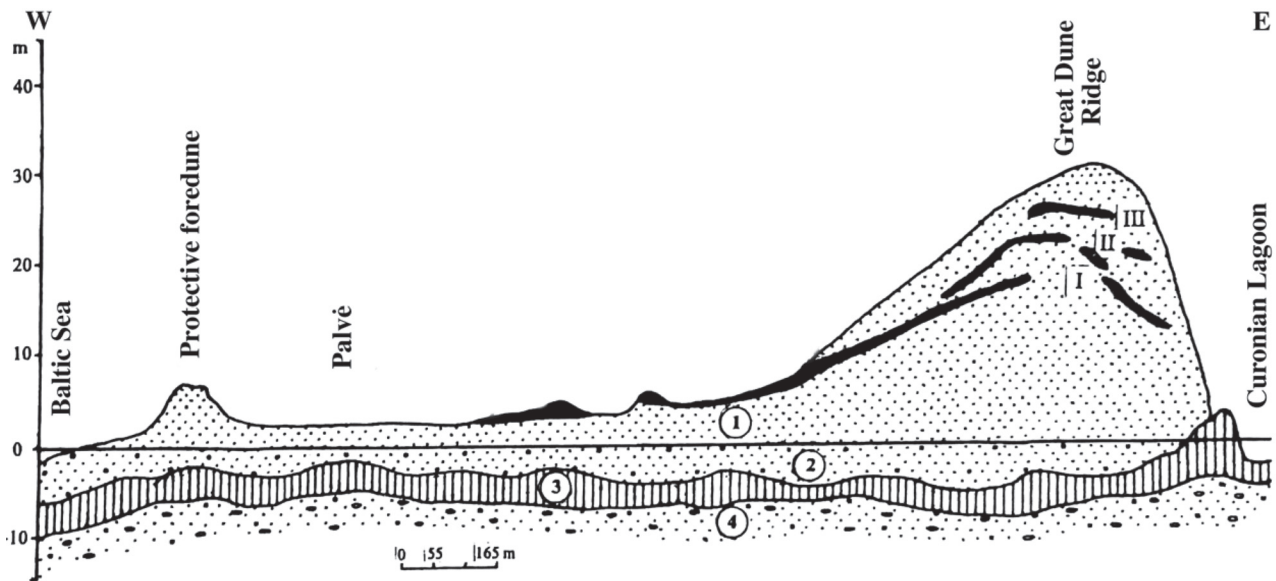


Fig. 8 The summary cross-section of the Curonian Spit in the W–E direction. 1 – fine-grain dune sands, 2 – older aeolian and marine sands, 3 – Curonian Lagoon organogenic sediments (carbonatic sapropel, lagoon marl), 4 – marine sand with pebbles and gravel; I, II, III – paleosols. Adapted from Gudelis (1993)

three separate zones with different activity regimes: 1) the accumulating E slope, 2) the eroding top and the W slope of the ridge, and 3) the inactive toe of the W slope. Česnulevičius *et al.* (2017) have also noted that the E slope of the ridge is more active.

The elevation change is mostly determined by the ridge altitudes. The absolute altitude was previously proposed as one of the main factors influencing the relief changes in the study area (Česnulevičius *et al.* 2006; Morkūnaitė 2000). In this study, this statement was supported by the observed elevation differences, as well as strong correlation coefficients (Table 4). The most pronounced elevation changes take place in the areas of highest elevations, which are mostly decreasing in height (Fig. 6d). It is probably related to the wind flow dynamics: as wind approaches a slope it is forced to accelerate (Hesp 2002; Lancaster 2009; Mckenna Neuman *et al.* 1997) which in turn results in a higher wind erosion capacity in higher regions. This relationship with the absolute altitude can also be explained by the groundwater table, which is closer to the surface in lower areas, thus providing favourable conditions for stabilising vegetation cover (Gonçalves, Henriques 2015; Povilanskas *et al.* 2006). Groundwater table also limits erosion depth, as wet sand is more coherent and harder for the wind to pick up and deflate (Hesp 2002). In the study area, Morkūnaitė *et al.* (2018) found the groundwater table to be 1–2 m deep on the toe of the W slope of the ridge and much deeper within the ridge itself, thus possibly relating to vegetation dominance on the westernmost, low-lying areas.

Smaller-scale relief forms can also be more exposed to winds compared to their surroundings, or

such exposed forms can modify wind patterns by forcing the wind gradient to increase in some places and to cease in others (Jackson *et al.* 2013). There are many discussions on the multiscale nature of geomorphological processes, e.g., on what scale relief changes should be analysed (Lancaster *et al.* 2013). This scale can be unique for each study site or even for each type of a relief form. In this study, the best-fitting radius to represent exposed relief forms relative to their surroundings seems to be close to 50 cells (100 m), as relative heights calculated using this radius yielded the highest correlation coefficients (Fig. 7). Elevation changes are inversely related to relative elevation. This means that areas lying higher than their surroundings are being deflated, while lower areas are more likely to be locations of sand accumulation. Such protruding relief forms are more vulnerable to winds from all directions, and they absorb much more momentum from the wind, while lower areas can be in the wind shadow zone, or the wind may decrease in velocity as wind streams separate after crossing a barrier (Hesp 2002). In addition, the bottoms of blowouts could be reaching groundwater levels and increasing the cohesiveness of sediments, making them harder to deflate (Beakawi Al-Hashemi, Baghabra Al-Amoudi 2018).

The correlation coefficient values calculated for slope *vs.* elevation difference were close to zero (Table 4). This is expected as steep slopes can be both a location of erosion (e.g., deflation scarps) and a location of accumulation (e.g., on the lee slope), and thus elevation difference can be both positive and negative. Nevertheless, slope is an important factor for elevation changes, as it can be concluded from

the found direct relationship (Fig. 6f): the steeper the slope is, the larger the elevation difference is. This can be explained by several mechanisms. Firstly, slope determines the energy required to initiate the transport of sand particles (Sherman, Li 2012; Van Dijk *et al.* 1999) and thus the threshold value of wind speed and energy for transport uphill. The transport on a steeper slope requires more energy compared to less steep or even declining surfaces (Iversen, Rasmussen 1994; Sherman, Li 2012). At the same time, steeper slopes have larger accelerating effects on the wind gradient. In addition, on much steeper slopes, aeolian processes are no longer the main factors for slope erosion: dry sand has an angle of repose of 34° (Beakawi Al-Hashemi, Baghabra Al-Amoudi 2018; Smyth, Hesp 2015), and slopes with higher inclinations are more vulnerable to gravitational processes (Iversen, Rasmussen 1994). Landslide formation has already been documented in the study area as a tsunami wave recorded in 1992 (Gudelis 1998; Povilanskas *et al.* 2006) and as fallen blocks of vegetation turf near steep slopes (Morkūnaitė 2000; Morkūnaitė, Česnulevičius 2005). Slope inclinations also have effects on trapping moisture within sediments, which controls the cohesion of sediments (Beakawi Al-Hashemi, Baghabra Al-Amoudi 2018; Van Dijk *et al.* 1999) and thus can shift the threshold value of repose angle, changing the boundary position between aeolian-gravitational processes (Nickling, Neuman 2009). Steeper slopes are mostly decreasing, although there is a slight peak around 35°, which could be related to sand accumulation on the lee slopes of blow-out lobes, as these slopes are close to repose angle. Stoss slopes of these lobes have gentler slopes. This may explain why there is a negative average of elevation difference with gentle slopes.

Another important slope parameter is the aspect, especially with regard to the predominant wind direction. In the study area, E slopes are the most active and accumulation predominantly takes place on these slopes, while less active, W-facing slopes, are mostly being deflated (Fig. 6e). As W winds are predominant in the study area, this distribution of deflation on W-facing slopes and accumulation on E slopes is the fundamental distribution of sand transport along the predominant wind direction: stoss (in our case W-facing) slope is being eroded, while on the lee (E-facing) slope sand accumulation takes place (Lancaster 2009) due to previously mentioned wind pattern changes forced by slope inclination. Interestingly, in the study area S- and SW-facing slopes appear to be more active than W-facing slopes. This is a common observation that S-facing slopes are more active. This is due to solar insolation, which dries S slopes more effectively, reducing moisture content in the sediments and thus lowering the sand cohesion

(Hesp 2011a; Hugenholtz, Wolfe 2006). Morkūnaitė (2000) has noted that most of the scarps in the study area are facing the SW direction, and it is evident that these slopes would have larger-scale changes due to additional effects of gravitational transport, thus leading to the negative average of elevation differences.

When comparing elevation differences within the same area, e.g., an active blowout or its depositional lobe, the intensity of elevation change depends on the time interval that has passed between measurements (Fig. 5). From this it can be concluded that these observed changes are rather directional. It is obvious that a larger elevation difference requires a longer interval of time. Differences throughout 12 years (2010–2022) were observed to range from 5 up to 15 m, while in 5 months (e.g., between May 2018 and Oct. 2018) the same location underwent only a fraction of these changes. Over a 12 years period (2010–2022), the average maximum elevation difference can reach the rates of approx. +/-1.3 m/year. Similar values were observed in the study area in 2003–2004; they ranged from 0.8–2.4 m for Nagliai and Vinkis dunes (Morkūnaitė, Česnulevičius 2005). However, even on a short-time scale, it is possible to note that summer and autumn months appear to be more active, as some areas reach more intense elevation changes (min and max values in Table 2). These months also have a more negative balance, which could be explained by the May–October months usually being the driest and the windiest months (Česnulevičius *et al.* 2006) and by the increased recreational load in the summer season, as many people come to visit the Nagliai Dune complex. In addition, in the winter months, there is usually snow cover, which shields the dunes from the wind (Česnulevičius *et al.* 2019; Hesp 2011b). During *DEMI801* acquisition, the ground was frozen, which also inhibited any sand deflation (Baughman *et al.* 2018). It was noted before that climate and meteorological conditions are important agents in dune dynamics (Abhar *et al.* 2015; Hesp 2002). Unfortunately, in the study area, there are no permanent meteorological stations, thus there are no direct climatic measurements that could have been included in this study.

To evaluate the balance of the whole system, it is best to compare two DEMs that are further apart in time, as on a shorter scale a measurement error can manifest more easily. Based on the average elevation difference in the bare-sand class (see Table 3), it is evident that dune elevation is decreasing in height by about 2 cm/year on average, while in some places it can reach up to +/-1.3 m/year. A negative balance in the system, which was already indicated by researchers, is linked with the lack of sediment supply from outside the system (Česnulevičius *et al.* 2006; Gudelis 1998; Mardosienė 1989; Povilanskas *et al.* 2006).

All our acquired measurements and calculated relationships can be used for the quantitative estimation and forecasting of relief changes in Pilkosios Dunes. Although there is a large complexity and uncertainty of the aeolian systems, it is possible to calculate an estimated future state of an absolute altitude for each location using regression curves presented in this study (Fig. 6) in combination with statistical and/or machine learning models derived from this and supplementary data (Andrews *et al.* www.elsevier.com/locate/geomorph; Smyth, Hesp 2015).

CONCLUSIONS

The DEMs of Pilkosios Dunes compiled in this study by using Lidar and UAV-aided photogrammetry present new high-quality morphometric data. This data enabled a quantitative evaluation of aeolian dynamics in this area during 2010–2022. The total balance of Pilkosios Dunes appeared to be negative, decrease in height rate was ~ 2 cm/year in the active part of the dunes, suggesting that sand was transported towards the shoreline of the Curonian Lagoon.

The acquired data also allowed analysis of environmental factors influencing aeolian morphodynamics in this area. The distance to the edge of grassland/bare-sand classes proved to be the most significant factor influencing dune dynamics in the active part of the dunes. The elevation changes were almost four times higher at distances further than 20 m from this edge compared to areas directly on the edge. The distance to the shoreline of the Curonian Lagoon was the second strongest factor. This factor allows distinguishing three sectors in the study area: 1) the adjacent E slope of the Great Dune Ridge, where sand accumulation takes place; 2) the middle and west slope of the ridge, where mostly deflation takes place; and 3) the furthest-away, low laying west sector, which appears to be relatively stable. Relative elevation inversely correlated with elevation difference. Calculations with different neighbourhood radii showed that the 50 cells neighbourhood is the most sensitive to elevation changes. The absolute altitude is directly related to the intensity of elevation change. There is a negative trend between slope and elevation change, indicating that the steepest slopes are the most vulnerable to elevation changes. However, this relationship was relatively weak as steep slopes can be both places of accumulation and of deflation. Eastern slopes tend to increase in height, while SW-W slopes are mostly being eroded.

The analytical derivatives calculated in this study enable the forecasting of aeolian morphodynamics of Pilkosios Dunes in the future, according to the surface class, proximity to the edge of surface classes, proximity to the Curonian Lagoon, absolute and relative elevation, slope, and slope direction. Such forecasts

would provide the basis for sensitive areas within Pilkosios Dunes and facilitate the selection of effective landscape managements strategies.

ACKNOWLEDGMENTS

Authors would like to express sincere appreciation to the two anonymous reviewers for their insightful comments. GT and LB were supported by S-MIP-21-9 “The role of spatial structuring in major transitions in macroevolution”.

REFERENCES

- Abhar, K.C., Walker, I.J., Hesp, P.A., Gares, P.A. 2015. Spatial-temporal evolution of aeolian blowout dunes at Cape Cod. *Geomorphology* 236, 148–162. <https://doi.org/10.1016/J.GEOMORPH.2015.02.015>
- Anderson, R.S. 1988. The pattern of grainfall deposition in the lee of aeolian dunes. *Sedimentology* 35 (2), 175–188. <https://doi.org/10.1111/J.1365-3091.1988.TB00943.X>
- Baughman, C.A., Jones, B.M., Bodony, K.L., Mann, D.H., Larsen, C.F., Himelstoss, E., Smith, J. 2018. Remotely Sensing the Morphometrics and Dynamics of a Cold Region Dune Field Using Historical Aerial Photography and Airborne LiDAR Data. *Remote Sensing* 10 (5), 792. <https://doi.org/10.3390/RS10050792>
- Beakawi Al-Hashemi, H.M., Baghabra Al-Amoudi, O.S. 2018. A review on the angle of repose of granular materials. *Powder Technology* 330, 397–417. <https://doi.org/10.1016/J.POWTEC.2018.02.003>
- Berendt, G. 1869. *Geologie des Kurischen Haffes und seiner Umgebung* [Geology of the Curonian Spit and its Surrounding]. Königsberg. [In German].
- Bučas, J. 2007. Kraštovarkinė problema Kuršių nerijoje [Land Management Problem in the Curonian Spit]. *Environmental Research, Engineering and Management* N (42), 70–80. [In Lithuanian].
- Buynevich, I. V., Bitinas, A., Pupienis, D. 2015. *Aeolian Sand Invasion: Georadar Signatures from the Curonian Spit Dunes, Lithuania*, 67–78. https://doi.org/10.1007/978-3-319-13716-2_5
- Česnulevičius, A., Izmailow, B., Morkūnaitė, R. 2006. Defliacinių daubų dinamika Kuršių nerijos Didžiajame kopagūbryje [The Dynamics of Deflation Basins in the Great Dune Ridge of the Curonian Spit]. *Geografija* 42, 21–28. [In Lithuanian].
- Česnulevičius, A., Morkūnaitė, R., Bautrenas, A., Bevainis, L., Ovodas, D. 2017. Intensity of geodynamic processes in the Lithuanian part of the Curonian Spit. *Earth System Dynamics* 8 (2), 419–428. <https://doi.org/10.5194/ESD-8-419-2017>
- Česnulevičius, A., Bautrenas, A.U., Bevainis, L., Mačiulevičiute-Turliene, N. 2019. Comparison of accuracy of UAV aeriels and ground measurements in the Curonian Spit dunes. *Baltic Journal of Modern Computing* 7 (4), 571–585. <https://doi.org/10.22364/BJMC.2019.7.4.10>

- Dobrotin, N., Bitinas, A., Michelevičius, D., Damušyte, A., Mažeika, J. 2013. Reconstruction of the Dead (Grey) Dune evolution along the Curonian Spit, Southeastern Baltic. *Bulletin of the Geological Society of Finland* 85 (1), 53–64. <https://doi.org/10.17741/BGSF/85.1.004>
- Fonstad, M.A., Dietrich, J.T., Courville, B.C., Jensen, J.L., Carbonneau, P.E. 2013. Topographic structure from motion: a new development in photogrammetric measurement. *Earth Surface Processes and Landforms* 38 (4), 421–430. <https://doi.org/10.1002/ESP.3366>
- Gares, P.A., Nordstrom, K.F. 1995. A Cyclic Model of Fore-dune Blowout Evolution for a Leeward Coast: Island Beach, New Jersey. *Annals of the Association of American Geographers* 85 (1), 1–20. <https://doi.org/10.1111/J.1467-8306.1995.TB01792.X>
- Gonçalves, J.A., Henriques, R. 2015. UAV photogrammetry for topographic monitoring of coastal areas. *ISPRS Journal of Photogrammetry and Remote Sensing* 104, 101–111. <https://doi.org/10.1016/j.isprsjprs.2015.02.009>
- Gudelis, V. 1993. *Jūros krantotyros terminų žodynas* [Glossary of Terms for Coastline Studies]. Academia. [In Lithuanian]
- Gudelis, V. 1998. *Lietuvos įjūris ir pajūris: monografija* [The Lithuanian Seaside and Coastline: Monography]. Vilnius, Spauda. [In Lithuanian].
- Gudelis, V., Michaliukaitė, E. 1959. Kuršių Nerijos dabartinių eolinių smėlių litologijos ir eolodinaminės diferenciacijos klausimu [On the Lithology and Eolodynamic Differentiation of the Present-Day Eolian Sands of the Curonian Spit]. *Geografinis Metraštis* 2, 535–564. [In Lithuanian].
- Guillot, B., Pouget, F. 2015. UAV Applications in Coastal Environment, Example of the Oleron Island for Dunes and Dikes Survey. *International Archives of the Photogrammetry, Remote Sensing and Spatial Information Sciences – ISPRS Archives* 3, 321–326. <https://doi.org/10.5194/ISPRSARCHIVES-XL-3-W3-321-2015>
- Hesp, P. 2002. Fore-dunes and blowouts: initiation, geomorphology and dynamics. *Geomorphology* 48 (1–3), 245–268. [https://doi.org/10.1016/S0169-555X\(02\)00184-8](https://doi.org/10.1016/S0169-555X(02)00184-8)
- Hesp, P. 2011a. Dune Coasts. In: Wolanski, E., McLusky, D. (Eds), *Treatise on Estuarine and Coastal Science* 3, 193–221. Waltham: Academic Press. <https://doi.org/10.1016/B978-0-12-374711-2.00310-7>
- Hesp, P. 2011b. Dune Coasts Drivers of coastal dune dynamics on the Younghusband Peninsula, South Australia. View project Coastal Blowout Dynamics at Cape Cod View project. *Treatise on Estuarine and Coastal Science* 3, 193–222. <https://doi.org/10.1016/B978-0-12-374711-2.00310-7>
- Hugenholtz, C.H., Wolfe, S.A. 2006. Morphodynamics and climate controls of two aeolian blowouts on the northern Great Plains, Canada. *Earth Surface Processes and Landforms* 31 (12), 1540–1557. <https://doi.org/10.1002/ESP.1367>
- Iversen, J.D., Rasmussen, K.R. 1994. The effect of surface slope on saltation threshold. *Sedimentology* 41 (4), 721–728. <https://doi.org/10.1111/J.1365-3091.1994.TB01419.X>
- Jackson, D., Cruz-Avero, N., Smyth, T., Hernández-Calvento, L. 2013. 3D airflow modelling and dune migration patterns in an arid coastal dune field. *Journal of Coastal Research* 165 (65 (10065)), 1301–1306. <https://doi.org/10.2112/SI65-220.1>
- Lancaster, N. 2009. Dune Morphology and Dynamics. *Geomorphology of Desert Environments* 557–595. https://doi.org/10.1007/978-1-4020-5719-9_17/COVER
- Lancaster, N., Baas, A.C., Sherman, D.J. 2013. Aeolian geomorphology: introduction. *Treatise on Geomorphology*, 1–6. Elsevier Academic Press.
- Le Mauff, B., Juigner, M., Ba, A., Robin, M., Launeau, P., Fattal, P. 2018. Coastal monitoring solutions of the geomorphological response of beach-dune systems using multi-temporal LiDAR datasets (Vendée coast, France). *Geomorphology* 304, 121–140. <https://doi.org/10.1016/j.geomorph.2017.12.037>
- Mardosienė, D. 1989. Kuršių nerijos pustomų kopų dinamika [The Curonian Spit Dune Dynamics]. *Geografinis Metraštis* 25–26, 29–44. [In Lithuanian].
- Mckenna Neuman, C., Lancaster, N., Nickling, W.G. 1997. Relations between dune morphology, air flow, and sediment flux on reversing dunes, Silver Peak, Nevada. *Sedimentology* 44 (6), 1103–1111. <https://doi.org/10.1046/J.1365-3091.1997.D01-61.X>
- Michaliukaitė, E. 1967. Kuršių nerijos krantų ir kopų dinamika per pastaruosius 100 metų [The dynamics of the Curonian Spit's Shores and Dunes Over the Last 100 Years]. *Geografinis Metraštis* 8, 97–117. [In Lithuanian].
- Moe, D., Savukynienė, N., Stančikaitė, M. 2005. A new 14C (AMS) date from former heathland soil horizons at Kuršių Nerija, Lithuania. *Baltica* 18 (1), 23–28.
- Morkūnaitė, R. 2000. Vėjo veiklos pasekmės Kuršių nerijos Juodkrantės–Pervalkos kopų ruože [Consequences of the Wind Activity in the Curonian Spit in the dunes in Juodkrantė–Pervalka stretch]. *Geografinis Metraštis* 33, 244–254. [In Lithuanian].
- Morkūnaitė, R., Česnulevičius, A. 2005. Changes in Blowout Segments of the Main Ridge in the Curonian Spit in 1999–2003. *Acta Zoologica Lituanica* 15 (2), 145–150. <https://doi.org/10.1080/13921657.2005.10512392>
- Morkūnaitė, R., Bautrėnas, A., Česnulevičius, A., Dobrotin, N., Baubinienė, A., Jankauskaitė, M., Kalesnikas, A., Mačiulevičiūtė-Turlienė, N. 2018. Changes in quantitative parameters of active wind dunes on the south-east Baltic Sea coast during the last decade (Curonian Spit, Lithuania). *Geological Quarterly* 62 (1), 38–47. doi: 10.7306/gq.1389. <https://doi.org/10.7306/GQ.1389>
- Nickling, W.G., Neuman, C.M.K. 2009. Aeolian sediment transport. *Geomorphology of Desert Environments*, 517–555. https://doi.org/10.1007/978-1-4020-5719-9_17/COVER
- Obilor, E.I., Amadi, E.C. 2018. Test for Significance of Pearson's Correlation Coefficient (r). *International Journal of Innovative Mathematics, Statistics & Energy Policies* 6 (11), 11–23. www.seahipaj.org

- Paškauskas, S. 2006. Morphometric investigations of the main dune ridge on the Curonian Spit, Lithuania. *Baltica 19 (1)*, 38–46.
- Povilanskas, R. 2009. Spatial diversity of modern geomorphological processes on a Holocene Dune Ridge on the Curonian Spit in the South-East Baltic. *Baltica 22 (2)*, 77–88.
- Povilanskas, R., Satkūnas, J., Taminskas, J. 2006. Results of cartometric investigations of dune morphodynamics on the Curonian Spit. *Geologija 53*, 22–27.
- Povilanskas, R., Baghdasarian, H., Arakelyan, S., Satkūnas, J., Taminskas, J. 2009. Secular Morphodynamic Trends of the Holocene Dune Ridge on the Curonian Spit (Lithuania/Russia). *Journal of Coastal Research 25 (1)*, 209–215. <https://doi.org/10.2112/07-0927.1>
- Pucino, N., Concurso, S. 2016. UAV Monitoring of Dune Dynamics – Anna Bay Entrance, Stockton Bight. *25th NSW Coastal Conference*.
- Savukyniene, N., Moe, D., Usaityte, D. 2003. The occurrence of former heathland vegetation in the coastal areas of the south-east Baltic Sea, in particular Lithuania: A review. *Vegetation History and Archaeobotany 12 (3)*, 165–175. <https://doi.org/10.1007/S00334-003-0008-5/FIGURES/5>
- Sherman, D.J., Li, B. 2012. Predicting aeolian sand transport rates: A reevaluation of models. *Aeolian Research 3 (4)*, 371–378. <https://doi.org/10.1016/J.AEOLIA.2011.06.002>
- Smyth, T.A.G., Hesp, P.A. 2015. Aeolian dynamics of beach scraped ridge and dyke structures. *Coastal Engineering 99*, 38–45. <https://doi.org/10.1016/J.COASTALENG.2015.02.011>
- Suo, C., McGovern, E., Gilmer, A. 2017. UAV data for coastal dune mapping. Abstracts of 10th International Conference “*Environmental Engineering*”, 27–28 April 2017, VGTU, Vilnius, 27–28. <https://doi.org/10.3846/enviro.2017.245>
- Taddia, Y., Corbau, C., Zambello, E., Russo, V., Simeoni, U., Russo, P., Pellegrinelli, A. 2017. Uavs to Assess the Evolution of Embryo Dunes. *The International Archives of Photogrammetry, Remote Sensing and Spatial Information Sciences 42*, 363–369. <https://doi.org/10.5194/ISPRS-ARCHIVES-XLII-2-W6-363-2017>
- Van de Ven, T.A.M., Fryrear, D.W., Spaan, W.P. 1989. Vegetation characteristics and soil loss by wind. *Journal of Soil and Water Conservation 44 (4)*, 347–349. <https://www.jswnonline.org/content/44/4/347>
- Van Dijk, P.M., Arens, S.M., Van Boxel, J.H. 1999. Aeolian processes across transverse dunes. II: modelling the sediment transport and profile development. *Earth Surface Processes and Landforms: The Journal of the British Geomorphological Research Group 24 (4)*, 319–333. [https://doi.org/10.1002/\(SICI\)1096-9837\(199904\)24:4](https://doi.org/10.1002/(SICI)1096-9837(199904)24:4)
- Wolfe, S.A., Nickling, W.G. 1993. The protective role of sparse vegetation in wind erosion. *Progress in Physical Geography 17 (1)*, 50–68. https://doi.org/10.1177/030913339301700104/ASSET/030913339301700104.FP.PNG_V03

Internet sources:

www.geoportal.lt

Andrews, B.D., Gares, P.A., Colby, J.D. *Techniques for GIS modeling of coastal dunes*. www.elsevier.com/locate/geomorph [Accessed 24 September 2023]